sustainability

MDPI

Article

Sustainable Biocomposites Based on Invasive *Rugulopteryx okamurae* Seaweed and Cassava Starch

Ismael Santana, Manuel Felix and Carlos Bengoechea *

Escuela Politécnica Superior, Universidad de Sevilla, Calle Virgen de África, 7, 41011 Sevilla, Spain; isantana@us.es (I.S.); mfelix@us.es (M.F.)
* Correspondence: cbengoechea@us.es

Abstract: The development of plastic materials based on cassava reduces the dependence on non-biodegradable petroplastics, and enhances the sustainability of the cassava value chain. In this sense, cassava starch (CS) is used as a reinforcer of biocomposites that also contain brown seaweed *Rugulopteryx okamurae* (RO). RO is an invasive species whose accumulation poses a strong environmental burden in the strait of Gibraltar. Because it can be used as a biopolymer, its use in the plastics industry would promote a healthy ecosystem. Thus, RO/CS mixtures with different RO/CS ratios (from 100/0 to 30/70) were processed through injection moulding at 140 °C. The thermal properties of plastic samples have been analysed through calorimetric, thermogravimetric and rheological techniques. Moreover, the mechanical properties, hydrophilicity, and microstructure of samples have also been studied. Thus, biopolymer degradation of the composites seems to happen at 213–303 °C, as revealed by thermal gravimetric analysis (TGA) of the samples, whereas an exothermic peak observed in DSC at 350–500 °C would be related to the degradation of organic compounds in anaerobic conditions. Rheological tests evidenced a softening of the RO/CS biocomposites when CS content increased in the formulation, so that elastic moduli dropped from 23.72 MPa in the 70/30 to 5.69 MPa for 30/70. However, RO/CS biocomposites became more resistant and deformable as CS content increased: maximum stress and strain at break increased from 78.2 kPa and 0.14% (70/30 system) to 580 kPa and 25.2% (30/70), respectively. Finally, no important differences were observed in their water uptake capacities or microstructures when increasing CS ratio in the mixture. As cassava starch can be extracted from agro-industrial wastes (i.e., cassava peel and bagasse), its use in biocomposites could be of great use for a more sustainable approach for plastic materials.

Keywords: *Rugulopteryx okamurae*; cassava starch; biocomposites; rheology; injection moulding

Citation: Santana, I.; Felix, M.; Bengoechea, C. Sustainable Biocomposites Based on Invasive *Rugulopteryx okamurae* Seaweed and Cassava Starch. *Sustainability* **2024**, *16*, 76. https://doi.org/10.3390/su16010076

Academic Editor: Paolo Mocellin

Received: 28 November 2023
Revised: 18 December 2023
Accepted: 19 December 2023
Published: 21 December 2023

1. Introduction

The United Nations adopted in 2015 the Sustainable Development Goals (SDGs) which, among other things, has the objective of ensuring that by 2030 all people enjoy peace and prosperity. The 12th SDG (Responsible Consumption and Production) focuses on the efficient management of shared natural resources, and the way toxic waste and pollutants are disposed. In this sense, plastics constitute the second largest petroleum application, after energy applications [1], although they are produced, used and disposed in a way that is quite harmful for the environment. Conventional plastics production reached 390.7 million tonnes in 2021, of which only 8.3% were recycled, and only 1.5% of the global plastic production corresponded to bioplastics (i.e., plastics that are biodegradable and/or made from renewable sources) [2,3]. In the EU, an average of 35.9 kg of plastic packaging waste per person was produced, of which only 39.7% was recycled. As plastic production is expected to triple by 2060, at the same time that the global amount of plastic waste continues to increase, this is of serious concern [4]. The main problems caused by the widespread use and production of plastics derived from petroleum are pollution and accumulation. The former is associated mostly with the different greenhouse gases produced during their

production, which contributes to global warming [5], and the latter to the fact that most conventional plastics are not biodegradable [6].

Bioplastics can be considered as replacements of conventional plastics in a strategy to reduce their negative environmental impact. Bioplastics production is expected to increase worldwide from around 2.2 million tonnes in 2022 to about 6.3 million tonnes in 2027 [7]. Among the bioplastics, biodegradable bioplastics account for 51.5% of the total, of which starch blends represent almost 35%. Starch is a renewable and biodegradable polysaccharide commonly found in plants, which can be produced on a large scale and at low cost [5,8]. It consists of glucopyranose, linked by 1,4 α-glycosidic bonds for linear amylose subunits, or by α-1,6-glycosidic bonds for branched amylopectin subunits [9,10]. The different subunits that form starch are strongly linked by hydrogen bonds, being able to form crystalline regions [10,11]. Cassava is widely cultivated in many tropical countries, making it a great source of cheap and accessible starch (cassava starch, CS) [12]. When starch originates from agro-industrial waste, the carbon footprint of bioplastics can be further reduced [13]. In this sense, wastes from the cassava starch industry (i.e., bagasse and, especially, peel) are alternative sources to commonly used commercial starch. Those wastes are generally discarded, resulting in serious environmental pollution [14]. Moreover, as CS has already displayed good mechanical properties, it could be considered as a reinforcer in biocomposites [15]. Previously, cassava starch has been used for the production of bioplastics through different techniques, such as extrusion [16] or casting [17], for various applications such as food packaging [18] or medical material [19].

On the other hand, the use of invasive species and flora for obtaining biopolymers and producing bioplastics has also been considered as a way to boost the development of sustainable products [20,21]. This is the case of *Rugulopteryx okamurae* (RO), a brown seaweed of the *Dictyotaceae* family originally from the northwestern Pacific Ocean [22]. In 2020, it was included in the Spanish catalogue of exotic invasive species and is considered potentially problematic in other European countries such as Portugal, Italy and Greece, among others, due to its adaptability and the risk of displacement of the existing biodiversity in the Mediterranean Sea [23,24]. Additionally, the accumulation of [16] algae in fishing nets is also causing significant losses in the local economy [25]. However, bioplastics based solely on RO displayed poor mechanical properties and could not be used in many applications as a substitute for currently used plastic materials [21,26]. Thus, the addition of reinforcers in the formulation of biocomposites can be used as a strategy to improve specific features required in certain applications.

The aim of the present work is to obtain sustainable bioplastics through the development and characterisation of biocomposites based on combinations of CS and RO, as filler and matrix, respectively. Glycerol (Gly) was used as plasticiser and Gly content was kept constant for all biocomposites at 50%, and then the effect of different RO/CS ratios (100/0, 70/30, 50/50 and 30/70) was assessed. All bioplastics have been obtained by injection moulding at 140 °C and different characterisation techniques have been employed (differential scanning calorimetry (DSC), thermal gravimetric analysis (TGA), dynamic mechanical analysis (DMA), tensile tests, water absorption and scanning electron microscopy (SEM)).

2. Materials and Methods

2.1. Materials

The brown seaweed *Rugulopteryx okamurae* (RO) used in this work was collected alive from the bay of Algeciras (Cádiz, Spain), and supplied by the Andalusian Institute for Agricultural, Fisheries and Organic Production Research and Training (IFAPA, Puerto Real, Spain). Once freeze-dried, the seaweed was ground in a kitchen blender (Ironmix, CECOTEC, Valencia, Spain) at room temperature (below 30 °C) and maximum speed in two stages of 1 min each. A D [3,4] mean diameter within a range of 10 to 100 μm was obtained for most of the particles (~90%). RO powder obtained contains soluble carbohydrates (8%), protein (10%), lipids (12%), ash (18%), and moisture (13%) [21].

Food grade CS was supplied by Bernesa S.A. (Buenos Aires, Argentina). The purity of the CS was around 92–98% *w*/*w*. Amylose and amylopectin content were around 19 and 80% *w*/*w* respectively, with a molecular weight of 8×10^2 kDa for amylose and 68×10^3 kDa for amylopectin.

Gly, used as a plasticiser, was supplied by Panreac Química S.A. (Castellas del Vallès, Spain).

Ground RO and CS powders were first mixed by hand for 5 min and then fed onto a Haake Polylab QC two-blade counter-rotating batch mixer (ThermoHaake, Karlsruhe, Germany). Glycerol was then added, and all the components (approximately 60 g) were mixed at room temperature for 10 min at 50 rpm, obtaining homogeneous blends with different RO/CS/Gly ratios: 50/0/50, 35/15/50, 25/25/50 and 15/35/50 for the comparison on biocomposites (RO/CS equal to 70/30, 50/50 and 30/70 for RO/CS/Gly ratios 35/15/50, 25/25/50 and 15/35/50, respectively); and 70/0/30 and 0/70/30 for the comparison of bioplastics based on a single biopolymer. The biocomposites blends obtained from the mixing stage were processed through injection moulding in a lab-scale Minijet Piston Injection Moulding System (ThermoHaake, Karlsruhe, Germany). The cylinder temperature was kept at 60 °C to facilitate the flow of the blends to the mould when they were injected at a pressure of 500 bar for 20 s. Injected samples were kept in the mould at 140 °C and 200 bars for 150 s, obtaining rectangular biocomposite probes of $1 \times 10 \times 60$ mm^3. Similar conditions were used in previous papers for bioplastics made from *Rugulopteryx okamurae* and Gly as plasticizer [21].

2.2. Methods

Fourier Transform Infrared Spectroscopy (FTIR)

The samples were treated to make a measurement with an ATR objective and to obtain the FTIR spectrum, a BRUKER spectrometer (Billerica, MA, USA) using a model Invenio X. The tests were carried out for wavenumbers between 400 and 4000 cm^{-1}, with a resolution of 4 cm^{-1}.

2.3. Thermal Analysis

The DMA850 rheometer (TA Instruments, Wakefield, MA, USA) was used for dynamic mechanical thermal analysis. Frequency sweep tests (from 0.1 to 1 Hz at a constant temperature of 25 °C) and temperature ramp tests (from 0 to 180 °C at a constant frequency of 1 Hz) were performed in tension mode using the clamp geometry for rectangular probes. Both frequency sweep and temperature ramp were performed within the linear viscoelastic region (LVR), previously determined by strain sweep tests at 1 Hz within the temperature interval studied.

Differential scanning calorimetry (DSC) and thermogravimetric analysis (TGA) were performed on the simultaneous DSC-TGA (SDT) Q600 instrument (TA Instruments, Wakefield, MA, USA). Thermal tests were carried out using a temperature ramp of 10 °C/min from 10 to 600 °C. Samples (5–10 mg of ground bioplastics) were placed in a platinum and non-hermetic capsule and purged with a nitrogen flow of 50 mL/min.

2.4. Tensile Tests

Stress–strain curves were obtained by tensile tests performed in the strain-controlled RSA3 rheometer (TA Instruments, Wakefield, MA, USA). Probes were deformed to fracture at a constant elongation rate of 1 mm·min^{-1} at room temperature. Young's modulus (E), maximum stress (σ_{max}) and strain at break (ε_{max}) were obtained from stress–strain curves. These tests were carried out according to the ISO 527-2 standard [27] using rectangular probes of $1 \times 10 \times 60$ mm^3.

2.5. Water Uptake Capacity (WUC) and Soluble Matter Loss (SML)

The absorbent properties of the biocomposites obtained were analysed using a modification of the ASTM D570 standard [28] to analyse the water absorption of plastic materials.

Briefly, bioplastics were dried at 50 °C for 24 h (w_1), then immersed in 100 mL of deionised water for 24 h (w_2) and finally lyophilised (w_3) (keeping the porous structure after water absorption). The samples were weighed in each stage. The WUC and SML were calculated using Equations (1) and (2):

$$WUC\ (\%) = \frac{(w_2 - w_3)}{w_3} \times 100 \quad (1)$$

$$SML\ (\%) = \frac{(w_1 - w_3)}{w_1} \times 100 \quad (2)$$

2.6. Scanning Electron Microscopy (SEM)

The freeze-dried biocomposites were analysed by SEM after the WUC test. The samples were cut into small pieces, then they were gold coated (Au–Pt coated, with a thickness of 11 nm) and examined by SEM using a ZEISS EVO instrument (Oberkochen, Germany). A working distance of 37.5 mm, an acceleration voltage of 10 kV, and a beam current of 86 pA were employed to obtain images at a magnification of 200×. Images were analysed using ImageJ imaging software version v1.53e. (Bethesda, MD, USA).

2.7. Statistical Analysis

To carry out the statistical analysis, STATGRAPHICS Centurion XVIII software (The Plains, VA, USA) was used. All measurements were carried out at least in triplicate. Significant differences ($p < 0.05$) are indicated in selected parameters by superscript letters.

3. Results

3.1. RO/Gly and CS/Gly Bioplastics

In order to evaluate the synergic effect between RO and CS, bioplastics based on solely one of the components were processed by injection moulding. Please note that the processing of CS/Gly at a 50/50 ratio was not possible due to the high flowability of the initial blend. Thus, for the comparison of both biomass sources, both bioplastics based on one single component, plus the plasticiser, contained an active matter/Gly ratio of 70/30. DMA and mechanical properties were analysed for these bioplastics.

The evolution of viscoelastic moduli, elastic (E′) and viscous modulus (E″), with temperature and frequency is shown in Figure 1A and 1B, respectively, for bioplastics based on RO/Gly and CS/Gly. In both systems, the elastic modulus (E′) is above the viscous modulus (E″), which implies a predominant elastic behaviour. In Figure 1A, when samples are initially heated, a decrease in viscoelastic moduli takes place for both systems, although RO bioplastic finally achieves a steady state from around 125 °C onwards. On the other hand, even if starch bioplastic also achieves a plateau region at lower temperatures (around 80 °C), an increase of viscoelastic moduli takes place at about 125 °C, eventually reaching a local maximum at ~150 °C. Thus, CS bioplastic goes through a thermal strengthening mechanism that does not happen for RO.

It should also be noted that the RO bioplastic possesses E′ and E″ values much higher than those of CS bioplastic (i.e., two orders of magnitude higher). This should be related to the greater effect of glycerol used in the bioplastic made of CS, which causes a higher softening due to a greater mobility of amylose and amylopectin chains from starch.

Figure 1B shows the evolution of E′ and E″ with frequency for the RO/Gly and CS/Gly 70/30 systems. An increase in the E′/frequency slope is observed in the CS system (0.24 ± 0.0049) compared to the RO system (0.16 ± 0.018). This indicates a greater dependence of the viscoelastic modulus on the frequency for the CS system, which is consistent with the lower values of the viscoelastic moduli.

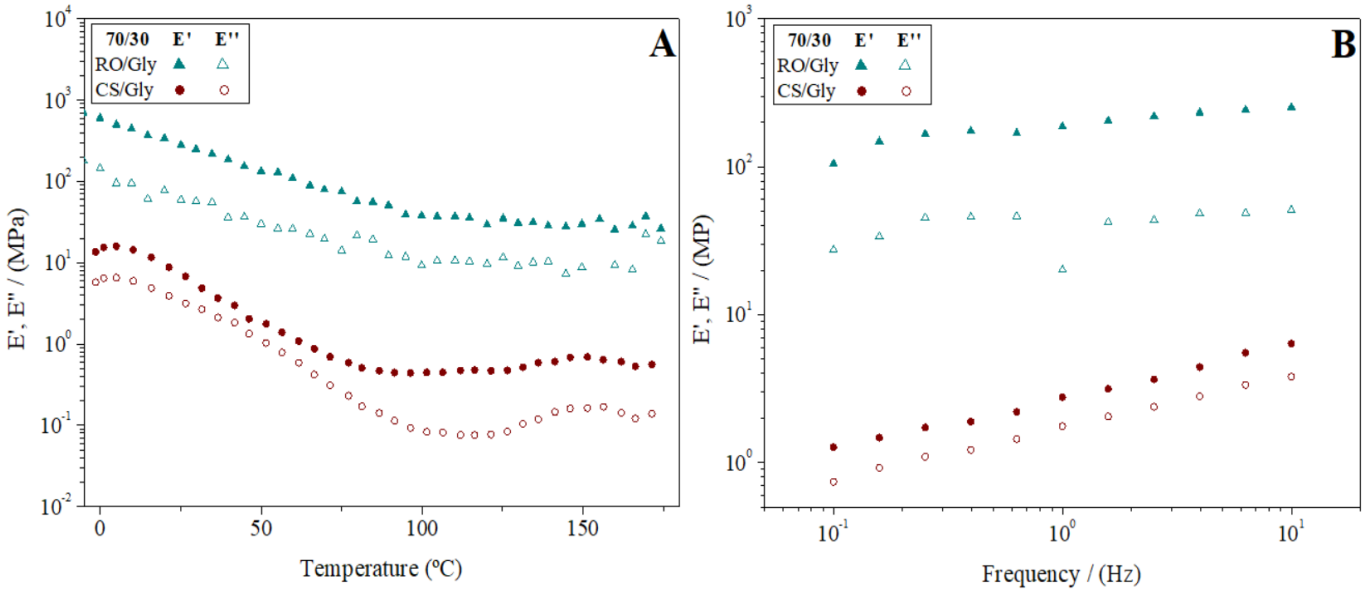

Figure 1. Evolution of elastic (E′) and viscous (E′′) moduli with temperature (**A**) and with frequency (**B**) for RO/Gly and CS/Gly bioplastics with 70/30 ratio.

In Table 1, the main mechanical properties of both bioplastics are included (E, σ_{max}, and ε_{max}). Young's modulus values agree with what was previously observed in DMA tests (Figure 1), while the E value of the RO/Gly system is two orders of magnitude higher than that of the CS/Gly system. RO/Gly also displays higher tensile strength, as denoted by its higher σ_{max} than that of CS/Gly system, which indicates that a greater application of stress is required to achieve the same deformation in the case of the RO/Gly bioplastic than in the CS/Gly bioplastic. On the other hand, the CS/Gly bioplastic shows a higher deformability (ε_{max}). Therefore, RO/Gly bioplastics are more resistant and rigid than CS/Gly bioplastic, but also more brittle.

Table 1. Mechanical parameters (Young's modulus (E), maximum strain (ε_{max}) and maximum stress (σ_{max})) of RO/Gly and CS/Gly bioplastics with a 70/30 ratio. Different letters above the same column indicate significant differences ($p < 0.05$).

System	E (kPa)	ε_{max} (%)	σ_{max} (kPa)
RO/Gly	$2.61 \times 10^3 \pm 5.14 \times 10^2$ a	$7.40 \times 10^{-1} \pm 1.20 \times 10^{-1}$ a	$6.79 \times 10^2 \pm 5.66 \times 10^1$ a
CS/Gly	$1.12 \times 10^1 \pm 7.57$ b	$5.64 \times 10^1 \pm 5.19$ b	$1.80 \times 10^2 \pm 4.59 \times 10^1$ b

3.2. RO/CS/Gly Biocomposites

3.2.1. Rheological Characterisation during Mixing of the Blends

Figure 2 shows the evolution of torque and temperature increase (ΔT, $\Delta T = T_{mixing} - T_0$) over mixing time for RO/CS/Gly biocomposites at different RO/CS ratios (100/0, 70/30, 50/50, 30/70 and 0/100). This figure shows a maximum value in torque for all systems processed at the beginning of the mixing stage. This maximum value is followed by a decrease until reaching a plateau region. These profiles are characteristic of heterogeneous blends (solid and liquid in this case), where the torque required during the mixing is higher at the beginning of the process until the plasticiser (Gly) covers the surface of the particles and acts as a lubricant [29]. Furthermore, there are no shear-induced cross-linking reactions apparent during mixing, which would have transformed the mixtures into very solid materials. On the other hand, homogeneous blends are eventually obtained that could still undergo cross-linking reactions during later stages. It should be noticed that the system with the highest CS content (RO/CS: 30/70) displays a greater increase in temperature. Moreover, no significant differences in torque were observed during the

mixing stage for CS-containing systems, with a difference of less than 1 N·m between them. On the other hand, the system with only RO (RO/CS: 100/0) displays the highest torque, peak temperature, and longer time to stabilise both parameters (i.e., torque and temperature). Thus, CS can be regarded as an additive that reduces the energy required for the first step in bioplastic processing. Moreover, the profiles obtained were similar to the ones observed for other bio-based blends, being suitable for their further processing by injection moulding [30].

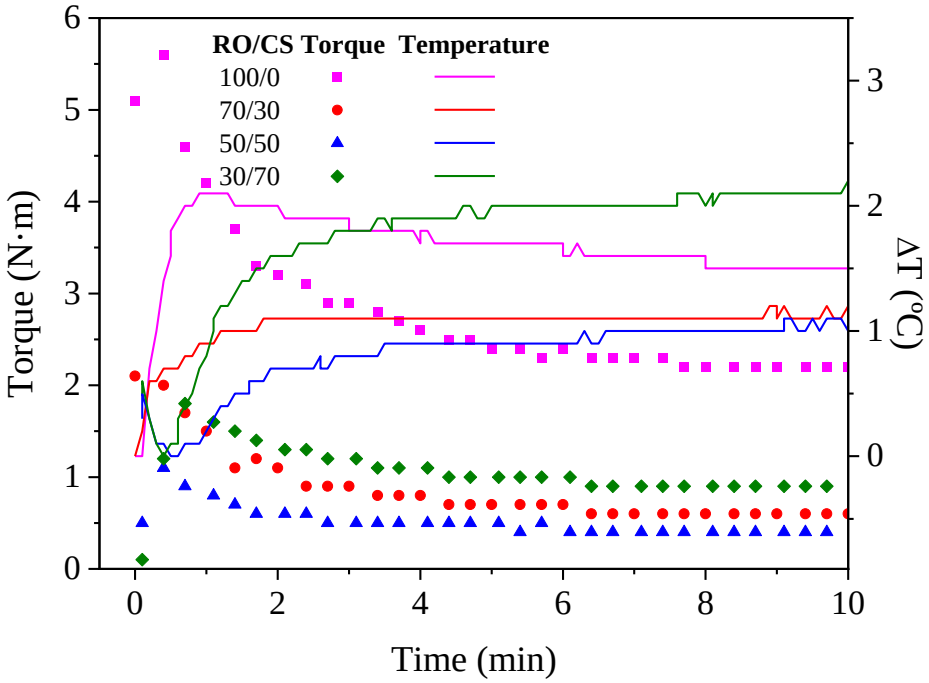

Figure 2. Torque and ΔT values over mixing time for different RO/CS/Gly systems (RO/CS ratios: 100/0, 70/30, 50/50 and 30/70) over the mixing stage.

3.2.2. FTIR of Biocomposites

FTIR spectra can be used to detect changes in molecular groups when variations in signals or their intensity occur [31], which may imply an interaction between different functional groups of different molecules [32]. Figure 3 shows the FTIR spectra of the CS and RO bioplastics separately, and that of the RO/CS/Gly biocomposite 25/25/50, so that possible interactions that occur between them can be detected. The peaks at higher wavelengths (3299–2930 cm^{-1}) correspond to free -OH and C-H stretching vibrations, respectively [33]. In comparison to individual bioplastics, the composite exhibits a profile strikingly similar to these materials, positioning itself at an intermediate standpoint. Notably, the bands at 574 and 1008 cm^{-1} in CS, corresponding to the stretching vibration of anhydro-glucose rings and C-O stretching, respectively, undergo a reduction in intensity and flattening when forming the composite. This phenomenon is mirrored in the most prominent peaks at approximately 1600 cm^{-1} and 1400 cm^{-1} in the RO. These peaks, associated with the vibrations of the O-C-O bond in the carboxylate group, signify asymmetric and symmetric stretching vibrations, respectively [34]. The former also includes a contribution from C-OH deformation vibrations, characteristic of alginates present in algae [35]. Other authors, such as Khalil et al. [33], have prepared biocomposites between starch and seaweed (*Kappaphycus alvarezii*), obtaining FTIR spectra and results quite similar to what was found in these RO and CS biocomposites.

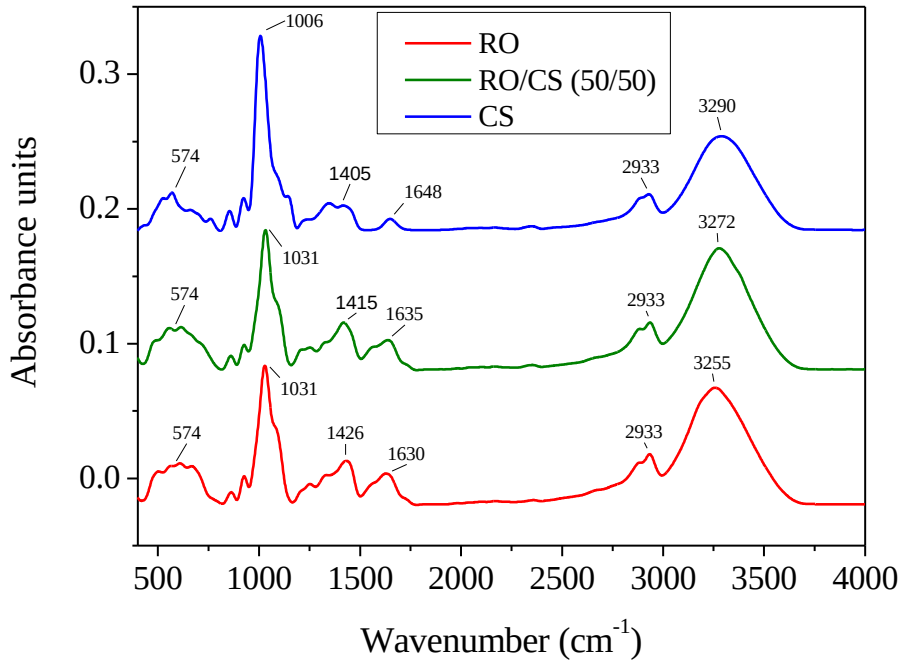

Figure 3. FTIR for the biocomposite with a RO/CS ratio 50/50 and bioplastics based solely on RO or CS.

FTIR of all biocomposites is supplied as Supplementary Figure S1.

3.2.3. Thermal Behaviour

- DSC and TGA

Figure 4 shows the DSC (Figure 4A) and TGA (Figure 4B) graphs obtained for RO/CS biocomposites with 100/0, 70/30, 50/50 and 30/70 ratios. The thermal profile obtained from the DSC test shows a thermal event corresponding to a T_g around 70 °C for all systems, which is cushioned for the lowest RO concentration. This T_g was previously reported for RO seaweed [21], where the addition of plasticiser (Gly) caused an anticipation of the peak in these systems. Contrary to the DSC of raw proteins, the endothermic peak caused by protein degradation is not observed. However, exothermic peaks were observed at 350–500 °C, corresponding to the degradation of organic compounds in the absence of O_2 [36].

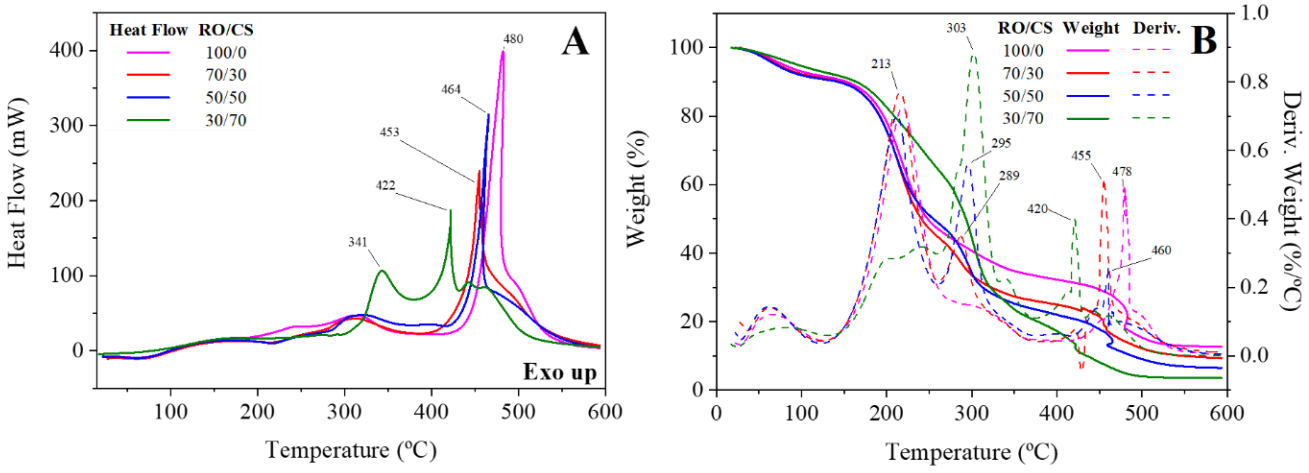

Figure 4. DSC (**A**) and TGA diagrams (**B**) of the bioplastics of RO/CS with 100/0, 70/30, 50/50 and 30/70 ratios from 20 to 600 °C.

Figure 4B shows the weight loss and the derivative of the weight loss as a function of temperature for all the RO/CS ratios studied in this work (100/0, 70/30, 50/50 and 30/70). The first peak observed for all systems before 100 °C corresponds to the loss of water.

In all systems, a group of peaks is observed that range between 200 and 215 °C as the CS content in the mixture increases (system 30/70 has a smaller peak as it has a lower amount of seaweed in the mixture). These peaks are mainly due to the decomposition of seaweed components (lipids, carbohydrates and proteins), losing around 70% of the mass [37]. The peaks around 300 °C correspond to the degradation of CS, and are therefore more notable in systems with a higher percentage of CS in the mixture, which agrees with the exothermic peak observed in Figure 3A [38]. From ~420 °C onwards, there is a succession of peaks in the derivative of weight loss with respect to temperature that increases with the percentage of RO in the mixture. This is indicative of the degradation of the rest of the volatile solid matter [39,40]. Similar results were obtained by Weerapoprasit et al. [41] for sodium alginate–cassava starch biocomposites. From these data it can be deduced that the processing temperature of bioplastics was suitable for these raw materials since it was below the degradation temperature of the components used for the manufacture of these biocomposites.

- DMA

Bioplastics were obtained from RO/GS/Gly blends by injection moulding at a mould temperature of 140 °C and 200 bar for 150 s. Figure 5A shows the temperature ramp tests obtained from DMA for bioplastics at 100/0, 70/30, 50/50, 30/70 and 0/100 RO/CS ratios. This figure shows that the value of E' is always higher than E", which implies that all biocomposites have a predominant elastic behaviour. This rheological response can be expected, confirming the successful formation of biocomposites under the processing conditions used. Moreover, a general decrease in E' and E" values is observed for all bioplastics under heating. This response is common in polymeric materials and it implies a disruption in hydrogen bonds produced by starch–starch interactions and other secondary starch–seaweed interactions, caused by an increase in temperature [42]. As no increase in viscoelastic moduli is observed in Figure 5A when heating, it can be confirmed that the thermosetting potential of the raw materials processed has been reached during the injection moulding stage of the blends (i.e., no further strengthening would be expected by increasing pressure or temperature). Thus, all samples tend to a steady value of E' at high temperatures (~150 °C). Figure 5B shows the influence of frequency on the E' and E" moduli for biocomposites at 100/0, 70/30, 50/50 and 30/70 RO/ratios. The response obtained is the typical of structured polymeric materials, where there is a certain dependence of the viscoelastic moduli on frequency [43]. It is remarkable how the slope (n) increases $(E'(\omega) = n{\cdot}\omega)$ when increasing CS in the mixture (~0.15 for RO/CS 100/0 and 70/30, ~0.19 for 50/50 and ~0.34 for 30/70), which implies a higher dependence on frequency when increasing the amount of CS. The behaviour denotes shorter relaxation times when CS is present in the biocomposite [44]. Moreover, the higher the percentage of CS in the mixture, the lower the viscoelastic moduli during the entire test. This is due to the marked decrease in the glass transition temperature of starch when a significant amount of plasticiser is added [11]. For example, Rodriguez-Gonzalez et al. [45] found that the T_g of starch decreased from 234 °C to −50 °C by adding 35% glycerol. Thus, this low T_g allows a higher mobility of the amylose and amylopectin that form the starch polymers, making it a softer and more deformable material and, therefore, causing a decrease in the viscoelastic moduli when increasing the percentage of CS in the RO/CS systems. Similar results are obtained by Lu et al., (2006) [46] for starch biocomposites with ramie crystallites as reinforcement, where an increase in the storage modulus is observed during the dynamic mechanical thermal analysis by increasing the percentage of ramie crystallites.

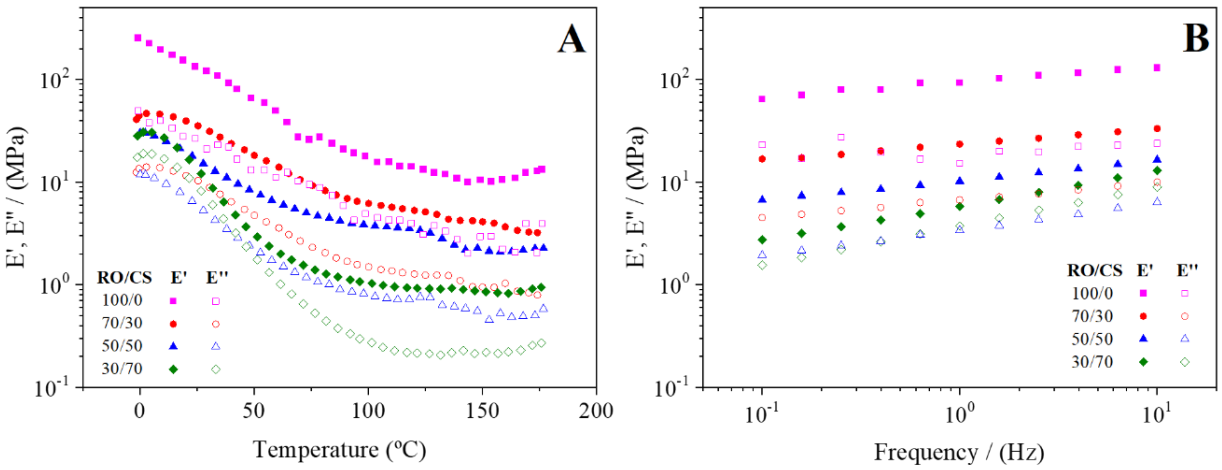

Figure 5. Evolution of elastic (E′) and viscous (E′′) moduli with temperature (**A**) and with frequency (**B**) for biocomposites at 100/0, 70/30, 50/50, 30/70 and 0/100 RO/CS ratios.

3.2.4. Mechanical Properties

Figure 6 shows the stress–strain curves obtained for biocomposites at 100/0, 70/30, 50/50 and 30/70 RO/CS ratios. A linear elastic region can be observed for all systems at the first stage of the mechanical test (i.e., at low strain). The slope corresponds to the Young's modulus (E). When a certain strain value is exceeded, the biocomposites begin to show plastic deformation, decreasing the slope of all systems. At a maximum stress value of stress (σ_{max}), the slopes of the systems analysed descend abruptly, as happens with the 30/70 RO/CS system, finishing with the breaking point of the material. In some cases, as in 50/50 and 70/30 RO/CS ratios, there is ductile rupture, where an extended deformation after maximum stress translates to a local deformation in the probe. In any case, the presence of CS in the biocomposites studied resulted in greater deformability, which should be directly related to the CS content. This greater deformability is accompanied by a decrease in the initial elastic slope. From these results, a fragile–ductile transition promoted by the presence of CS can be distinguished, being fragile when CS is absent from the formulation and ductile when CS is at the highest level.

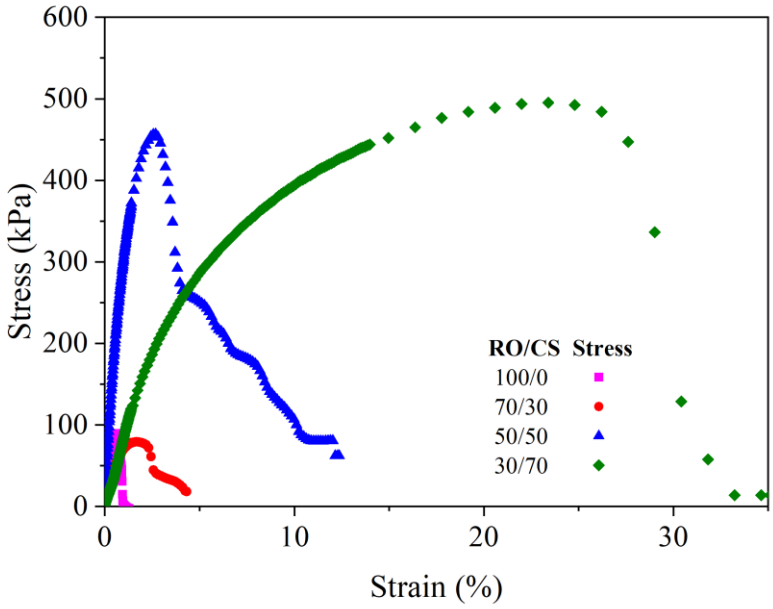

Figure 6. Stress–strain curves for biocomposites with different RO/CS ratios (100/0, 70/30, 50/50 and 30/70).

Parameters obtained from tensile tests (E, ε_{max} and σ_{max}) of RO/CS biocomposites (100/0, 70/30, 50/50 and 30/70) are shown in Table 2. No significant differences were observed for E values. The main difference between systems is observed in ε_{max} and σ_{max}. Both parameters increase when increasing CS percentage on the mixture. This result agrees with DMA tests, where softer materials with higher polymer mobility were deduced. The softening of the biocomposites can be attributed to Gly as plasticiser in the mixture, that produces an increase in the mobility of the biopolymer chains that forms the RO/CS based composites. Consequently, higher values of ε_{max} are observed when increasing CS in the RO/CS ratio, leading to a remarkable increase of one order of magnitude (from $1.98 \pm 3.20 \times 10^{-1}$% to $2.52 \times 10^{1} \pm 2.63$%) when increasing RO/CS from 50/50 to 30/70 and two orders of magnitude with respect to the bioplastic without CS (from 4.90×10^{-1}% $\pm 7.00 \times 10^{-2}$ to $2.52 \times 10^{1} \pm 2.63$%). Thus, higher contents of CS make biocomposites more ductile, obtaining biocomposites that present a higher σ_{max} value (from 8.80 ± 2.10 kPa to $5.80 \times 10^{2} \pm 9.37 \times 10^{1}$ kPa) the more CS there is in the mixture. This reduction in tensile strength produced when the Gly/CS ratio is high was also exhibited by Zanela. et al. [47] for bioplastics made of CS, PVA and glycerol and by Santana et al. [48] for cassava starch and glycerol bioplastics [49].

Table 2. Parameters from tensile tests (Young's modulus (E), maximum strain (ε_{max}) and maximum stress (σ_{max}) for biocomposites containing a RO/CS ratio of 100/0, 70/30, 50/50 and 30/70. Different superscript letters within the same column indicate significant differences ($p < 0.05$).

RO/CS	E (kPa)	ε_{max} (%)	σ_{max} (kPa)
100/0	$4.0 \times 10^{2} \pm 1.40 \times 10^{2}$ [a]	$4.90 \times 10^{-1} \pm 7.00 \times 10^{-2}$ [a]	$8.80 \times 10^{1} \pm 2.10 \times 10^{1}$ [a]
70/30	$1.71 \times 10^{2} \pm 9.41 \times 10^{1}$ [a]	$1.43 \pm 8.40 \times 10^{-1}$ [b]	$7.82 \times 10^{1} \pm 4.42 \times 10^{1}$ [a]
50/50	$4.25 \times 10^{2} \pm 4.72 \times 10^{1}$ [a]	$1.98 \pm 3.20 \times 10^{-1}$ [b]	$3.00 \times 10^{2} \pm 1.36 \times 10^{2}$ [c]
30/70	$2.67 \times 10^{2} \pm 1.96 \times 10^{2}$ [a]	$2.52 \times 10^{1} \pm 2.63$ [c]	$5.80 \times 10^{2} \pm 9.37 \times 10^{1}$ [d]

3.2.5. Water Uptake

Figure 7 shows the dependence of water uptake capacity (WUC) and soluble matter loss (SML) on the RO/CS biocomposite ratios (100/0, 70/30, 50/50 and 30/70). No significant differences were observed for the WUC values when increasing the amount of CS in the system, obtaining values between 250 and 300% approximately in all cases. This implies that the softening of the material (observed in due to the higher amount of Gly in relation to the CS) does not affect the WUC of the material, resulting in a higher mobility of the polymers that form the biocomposites without increasing the absorption pathways in its structure required for water absorption, which means that substitution of the biopolymer does not affect its WUC and that interactions that limit said water uptake capacity do not develop [50]. Although the WUC obtained does not lead to absorbent materials, the values reached make these materials suitable for absorbent materials, being the possible carrier of components to be released [51].

Regarding the SML, a small significant difference is observed in the systems with CS in the mix, where a small decrease in their values occurs. RO/CS 100/0, 70/30 and 50/50 systems display an SML between ~50–60%, corresponding mainly to the percentage of Gly present in the mixtures (50%). On the other hand, system with a RO/CS ratio of 30/70 displays a lower SML value, (41.16 ± 2.27%). This effect is produced because of the hydrophilic behaviour of Gly that can be released when the probes are immersed in water [52]. The remaining percentage lost is mainly due to the loss of part of the mass corresponding to the seaweed and starch. As this percentage is lower for the RO/CS 70/30, 50/50 and 30/70 systems, it is obvious that this remaining percentage loss is mainly due to the loss of seaweed. This agrees with the data obtained in the tensile tests, indicating a greater stability in the structure with CS present.

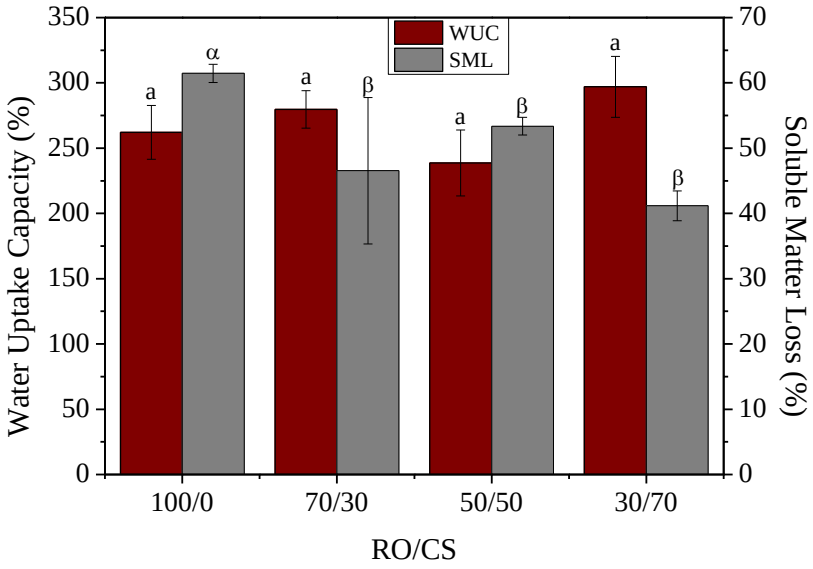

Figure 7. Water uptake capacity (WUC) and soluble matter loss (SML) for RO/CS systems at 100/0, 70/30, 50/50 and 30/70 ratios. Different letters above the same column indicate significant differences ($p < 0.05$).

3.2.6. Scanning Electron Microscopy (SEM)

Figure 8 shows the images obtained by SEM microscopy of biocomposites studied (100/0, 70/30, 50/50 and 30/70 RO/CS ratios) processed after water immersed tests over 24 h and subsequent freeze-drying.

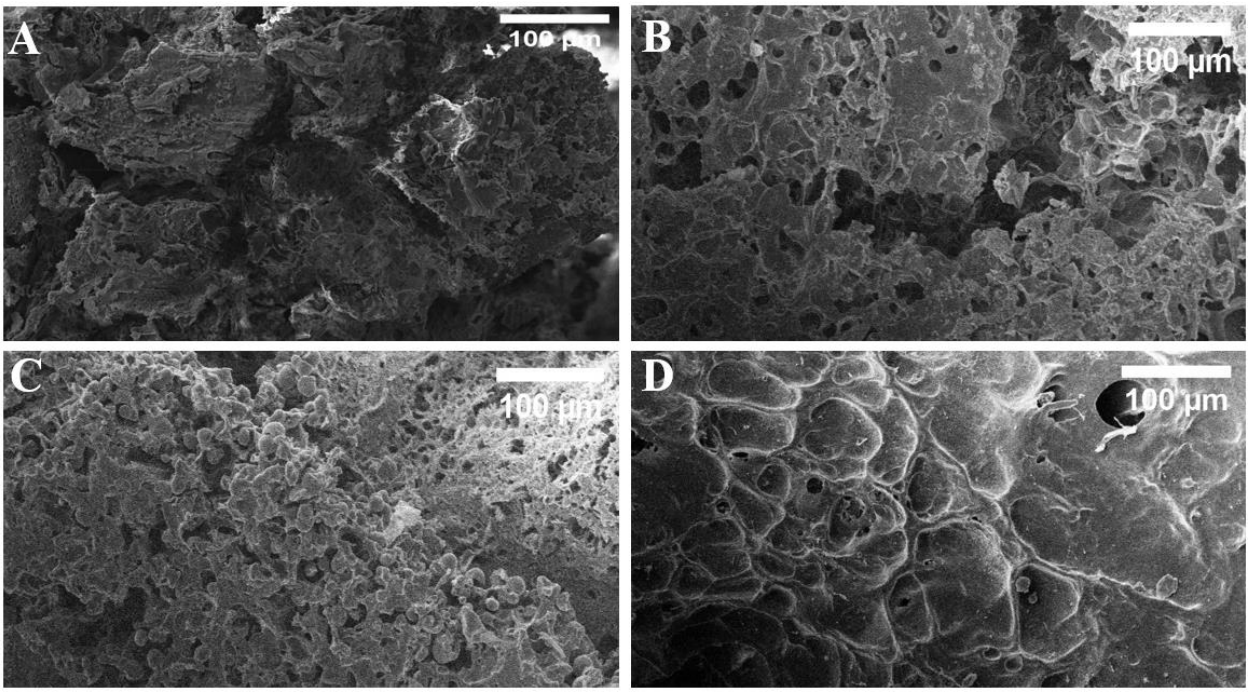

Figure 8. SEM images of biocomposites after water immersion and subsequent freeze drying at four RO/CS ratios: 100/0 (**A**), 70/30 (**B**), 50/50 (**C**) and 30/70 (**D**).

Figure 8 evidenced a softening of the structure when increasing the amount of CS in the mixture. Thus, when no CS was included in the formulation (Figure 8A), the surface is rough, and several cracks can be detected on the surface. The presence of CS (Figure 8B–D) promoted a more homogeneous surface. This was also observed by Ahmad

et al. [40] for sago starch and glycerol bioplastics. This is observed in Figure 8D, which corresponds to the 30/70 RO/CS system, where a smoother surface is observed compared to the other systems. This difference is less remarkable as the percentage of CS is reduced: for example, there is not a big structural difference observable between system RO/CS 70/30 (Figure 8B) and RO/CS 50/50 (Figure 8C). This smoother and more compact surface is consistent with the increase in the mechanical properties of biocomposites, obtaining more resistant biocomposites (Figure 6 and Table 2). On the other hand, more irregularities in the structure of systems with less or no CS results in more brittle biocomposites. Similar results were obtained by Ferreira et al., (2015) [53] for starch bioplastics with glycerol and poly(lactic acid).

4. Conclusions

When comparing RO/Gly and CS/Gly with a ratio of 70/30 separately, we saw an increase of two orders of magnitude of RO/Gly with respect to the CS/Gly bioplastic in the viscoelastic moduli. However, both show a decrease in the viscoelastic moduli when increasing temperature. In addition, RO/Gly bioplastic presents a higher Young's modulus and maximum stress, with a lower maximum strain value than CS/Gly, which implies that RO/Gly is a more brittle and rigid bioplastic.

When combining RO and CS at different RO/CS ratios (100/0, 70/30, 50/50 and 30/70), keeping always with 50/50 biomass/Gly ratio, DSC and TGA showed that the degradation of most components of the seaweed and of cassava starch was produced at 200–300 °C. From 410 °C onwards, the degradation of the volatile solid remains occurred. These peaks appeared at higher temperatures as the amount of seaweed in the mixture increased. The same evolution was observed in the final mass corresponding to the remaining solid residue after reaching 600 °C in the TGA, going from ~2% in the RO/CS 30/70 system to more than 10% in the 100/0 system. DMA showed a decrease of viscoelastic moduli when increasing CS in the mixture, all displaying a decrease of viscoelastic moduli when increasing temperature and a predominantly elastic behaviour. Regarding mechanical parameters, maximum strain, and stress increase were observed when increasing CS in the mixture, going from a maximum strain and stress of ~0.14% and 78.2 kPa, respectively for the RO/CS 70/30 ratio to ~25.2% and 580 kPa, respectively for the RO/CS 30//70 ratio. No remarkable differences were observed in the WUC values between the systems analysed. The only significant difference was related to the SML in the 100/0 RO/CS system, where the higher percentage (~62%) corresponded to the loss of Gly and part of the soluble components of the seaweed used. The rest of the composites displayed a loss of ~40–55% mainly due to the loss of Gly. Finally, a smoothing of the surface of the biocomposites when increasing the amount of CS in the mixture was noticed in the SEM images, being remarkable for the 30/70 RO/CS ratio system. This more compact structure acted to the benefit of its mechanical properties while no increase in the absorption of water was observed.

The production of biocomposites based on invasive seaweed species and cassava starch from biowastes would enhance sustainability in the plastic industry, reducing some environmental risks (e.g., displacement of local species, plastic accumulation).

Supplementary Materials: The following supporting information can be downloaded at: https://www.mdpi.com/article/10.3390/su16010076/s1, Figure S1: FTIR for all RO/CS biocomposites (RO/CS ratios: 100/0, 70/30, 50/50, 30/70 and 0/100).

Author Contributions: Conceptualization, M.F. and C.B.; methodology, M.F.; software, I.S.; validation, M.F. and C.B.; formal analysis, I.S.; investigation, I.S.; resources, C.B.; data curation, I.S.; writing—original draft preparation, I.S.; writing—review and editing, M.F. and C.B.; visualization, M.F. and C.B.; supervision, M.F. and C.B.; project administration, C.B.; funding acquisition, C.B. All authors have read and agreed to the published version of the manuscript.

Funding: The authors acknowledge the project PID2021-124294OB-C21 funded by MCIN/AEI/10.13039/501100011033/and by "ERDF A way of making Europe" for supporting this study, and the Andalu-

sian government and the European commission for funding the contract of Ismael Santana through the Youth Employment Initiative (EJ5-13-1).

Institutional Review Board Statement: Not applicable.

Informed Consent Statement: Not applicable.

Data Availability Statement: Data will be available under request.

Acknowledgments: The authors would also like to thank Ismael Hachero from the Andalusian Institute for Agricultural, Fisheries and Organic Production Research and Training (IFAPA, Puerto Real, Spain), and IFAPA itself, for providing the seaweed used in this work, and also the CITIUS for granting access and assistance with the microscopy and the functional characterisation services.

Conflicts of Interest: The authors declare no conflict of interest.

References

1. Mekonnen, T.; Mussone, P.; Khalil, H.; Bressler, D. Progress in bio-based plastics and plasticizing modifications. *J. Mater. Chem. A* **2013**, *1*, 13379–13398. [CrossRef]
2. Ashter, S.A. Introduction. In *Introduction to Bioplastics Engineering*; Elsevier: Amsterdam, The Netherlands, 2016; pp. 1–17, ISBN 9780323393966.
3. PlasticEurope: Plastics—The Facts 2022, H. Available online: https://plasticseurope.org/knowledge-hub/plastics-the-facts-2022 (accessed on 16 December 2022).
4. European Commission Reducing Plastic Pollution: Negotiations towards a New Global Instrument to Combat Plastic Pollution Advance. Available online: https://environment.ec.europa.eu/news/negotiations-towards-new-global-instrument-combat-plastic-pollution-advance-2023-11-20_en (accessed on 28 November 2023).
5. Atiwesh, G.; Mikhael, A.; Parrish, C.C.; Banoub, J.; Le, T.A.T. Environmental impact of bioplastic use: A review. *Heliyon* **2021**, *7*, e07918. [CrossRef] [PubMed]
6. Tokiwa, Y.; Calabia, B.P.; Ugwu, C.U.; Aiba, S. Biodegradability of plastics. *Int. J. Mol. Sci.* **2009**, *10*, 3722–3742. [CrossRef] [PubMed]
7. European Bioplastics Bioplastics Market Data. Available online: https://www.european-bioplastics.org/market/ (accessed on 28 November 2023).
8. Okada, M. Chemical syntheses of biodegradable polymers. *Prog. Polym. Sci.* **2002**, *27*, 87–133. [CrossRef]
9. Jariyasakoolroj, P.; Leelaphiwat, P.; Harnkarnsujarit, N. Advances in research and development of bioplastic for food packaging. *J. Sci. Food Agric.* **2020**, *100*, 5032–5045. [CrossRef] [PubMed]
10. Mottiar, Y.; Altosaar, I. Iodine sequestration by amylose to combat iodine deficiency disorders. *Trends Food Sci. Technol.* **2011**, *22*, 335–340. [CrossRef]
11. Zhang, Y.; Rempel, C.; Liu, Q. Thermoplastic Starch Processing and Characteristics-A Review. *Crit. Rev. Food Sci. Nutr.* **2014**, *54*, 1353–1370. [CrossRef]
12. Parra, D.F.; Tadini, C.C.; Ponce, P.; Lugao, A.B. Mechanical properties and water vapor transmission in some blends of cassava starch edible films. *Carbohydr. Polym.* **2004**, *58*, 475–481. [CrossRef]
13. Chan, J.X.; Wong, J.F.; Hassan, A.; Zakaria, Z. Bioplastics from agricultural waste. In *Biopolymers and Biocomposites from Agro-Waste for Packaging Applications*; Elsevier: Amsterdam, The Netherlands, 2021; pp. 141–169.
14. Weligama Thuppahige, V.T.; Moghaddam, L.; Welsh, Z.G.; Wang, T.; Xiao, H.-W.; Karim, A. Extraction and characterisation of starch from cassava (Manihot esculenta) agro-industrial wastes. *LWT* **2023**, *182*, 114787. [CrossRef]
15. Pavlath, A.E.; Robertson, G.H. Biodegradable polymers vs. recycling: What are the possibilities. *Crit. Rev. Anal. Chem.* **1999**, *29*, 231–241. [CrossRef]
16. Ezeoha, S.L. Production of Biodegradable Plastic Packaging Film from Cassava Starch. *IOSR J. Eng.* **2013**, *3*, 14–20. [CrossRef]
17. Oluwasina, O.O.; Olaleye, F.K.; Olusegun, S.J.; Oluwasina, O.O.; Mohallem, N.D.S. Influence of oxidized starch on physicomechanical, thermal properties, and atomic force micrographs of cassava starch bioplastic film. *Int. J. Biol. Macromol.* **2019**, *135*, 282–293. [CrossRef] [PubMed]
18. Oluwasina, O.O.; Akinyele, B.P.; Olusegun, S.J.; Oluwasina, O.O.; Mohallem, N.D.S. Evaluation of the effects of additives on the properties of starch-based bioplastic film. *SN Appl. Sci.* **2021**, *3*, 421. [CrossRef]
19. Arrieta, A.A.; Gañán, P.F.; Márquez, S.E.; Zuluaga, R. Electrically conductive bioplastics from cassava starch. *J. Braz. Chem. Soc.* **2011**, *22*, 1170–1176. [CrossRef]
20. Willett, K.; Howell, B. Using local invasive species and flora to manufacture collagen based biodegradable plastic tableware. In *Proceedings of the International Conference on Engineering Design, ICED*; The University of British Columbia: Vancouver, BC, Canada, 2017; Volume 1, pp. 151–158.
21. Santana, I.; Félix, M.; Guerrero, A.; Bengoechea, C. Processing and Characterization of Bioplastics from the Invasive Seaweed *Rugulopteryx okamurae*. *Polymers* **2022**, *14*, 355. [CrossRef] [PubMed]

22. Agatsuma, Y.; Kuwahara, Y.; Taniguchi, K. Life cycle of *Dilophus okamurae (Phaeophyceae)* and its associated invertebrate fauna in Onagawa Bay, Japan. *Fish. Sci.* **2005**, *71*, 1107–1114. [CrossRef]
23. García-Gómez, J.C.; Florido, M.; Olaya-Ponzone, L.; Rey Díaz de Rada, J.; Donázar-Aramendía, I.; Chacón, M.; Quintero, J.J.; Magariño, S.; Megina, C. Monitoring Extreme Impacts of Rugulopteryx okamurae (Dictyotales, Ochrophyta) in El Estrecho Natural Park (Biosphere Reserve). Showing Radical Changes in the Underwater Seascape. *Front. Ecol. Evol.* **2021**, *9*, 1–18. [CrossRef]
24. Altamirano Jeschke, M.; Zanolla, M. *Análisis de Riesgos de la Macroalga Exótica Rugulopteryx okamurae.*; Ministerio para la Transición Ecológica y Reto Demográfico: Madrid, Spain, 2019; p. 69.
25. García-Gómez, J.C.; Sempere-Valverde, J.; González, A.R.; Martínez-Chacón, M.; Olaya-Ponzone, L.; Sánchez-Moyano, E.; Ostalé-Valriberas, E.; Megina, C. From exotic to invasive in record time: The extreme impact of *Rugulopteryx okamurae* (Dictyotales, Ochrophyta) in the strait of Gibraltar. *Sci. Total Environ.* **2020**, *704*, 2. [CrossRef]
26. Zhang, C.; Show, P.L.; Ho, S.H. Progress and perspective on algal plastics—A critical review. *Bioresour. Technol.* **2019**, *289*, 121700. [CrossRef]
27. *ISO ISO 527-2*; Determination of Tensile Properties of Plastics—Test Conditions for Moulding and Extrusion Plastics. International Organization for Standardization: Geneva, Switzerland, 1996; Volume 2, p. 9.
28. *D570 ASTM D 570—98*; Standard Test Method for Water Absorption of Plastics. ASTM International—Standards Worldwide: West Conshohocken, PA, USA, 1985.
29. Jones, A.; Mandal, A.; Sharma, S. Protein-based bioplastics and their antibacterial potential. *J. Appl. Polym. Sci.* **2015**, *132*, 18. [CrossRef]
30. Felix, M.; Romero, A.; Cordobes, F.; Guerrero, A. Development of crayfish bio-based plastic materials processed by small-scale injection moulding. *J. Sci. Food Agric.* **2015**, *95*, 679–687. [CrossRef] [PubMed]
31. Wanchoo, R.K.; Sharma, P.K. Viscometric study on the compatibility of some water-soluble polymer-polymer mixtures. *Eur. Polym. J.* **2003**, *39*, 1481–1490. [CrossRef]
32. Xu, X.; Li, B.; Kennedy, J.F.; Xie, B.J.; Huang, M. Characterization of konjac glucomannan-gellan gum blend films and their suitability for release of nisin incorporated therein. *Carbohydr. Polym.* **2007**, *70*, 192–197. [CrossRef]
33. Khalil, A.; Khalil, H.P.S.A.; Yap, S.W.; Tye, Y.Y.; Tahir, P.M.; Rizal, S.; Nurul Fazita, M.R. Effects of Corn Starch and Kappaphycus alvarezii Seaweed Blend Concentration on the Optical, Mechanical, and Water Vapor Barrier Properties of Composite Films. *BioResources* **2018**, *13*, 1157–1173.
34. Flórez-Fernández, N.; Domínguez, H.; Torres, M.D. A green approach for alginate extraction from Sargassum muticum brown seaweed using ultrasound-assisted technique. *Int. J. Biol. Macromol.* **2019**, *124*, 451–459. [CrossRef] [PubMed]
35. Fenoradosoa, T.A.; Ali, G.; Delattre, C.; Laroche, C.; Petit, E.; Wadouachi, A.; Michaud, P. Extraction and characterization of an alginate from the brown seaweed *Sargassum turbinarioides Grunow*. *J. Appl. Phycol.* **2010**, *22*, 131–137. [CrossRef]
36. López-González, D.; Avalos Ramirez, A.; Ghorbel, L.; Rouissi, T.K.; Brar, S.; Giroir-Fendler, A.; Godbout, S.; Palacios, J.; Sanchez Silva, L.; Luis Valverde, J. Valorization of compost from animal breeding via pyrolysis and combustion. *Am. Soc. Agric. Biol. Eng.* **2014**, *1*, 141913285.
37. Marcilla, A.; Gómez-Siurana, A.; Gomis, C.; Chápuli, E.; Catalá, M.C.; Valdés, F.J. Characterization of microalgal species through TGA/FTIR analysis: Application to *nannochloropsis sp*. *Thermochim. Acta* **2009**, *484*, 41–47. [CrossRef]
38. Ma, X.; Yu, J.; Kennedy, J.F. Studies on the properties of natural fibers-reinforced thermoplastic starch composites. *Carbohydr. Polym.* **2005**, *62*, 19–24. [CrossRef]
39. Ma, X.; Chang, P.R.; Yu, J.; Stumborg, M. Properties of biodegradable citric acid-modified granular starch/thermoplastic pea starch composites. *Carbohydr. Polym.* **2009**, *75*, 1–8. [CrossRef]
40. Ahmad, Z.; Anuar, H.; Yusof, Y. The study of biodegradable thermoplastics sago starch. *Key Eng. Mater.* **2011**, *471–472*, 397–402. [CrossRef]
41. Weerapoprasit, C.; Prachayawarakorn, J. Properties of biodegradable thermoplastic cassava starch/sodium alginate composites prepared from injection molding. *Polym. Compos.* **2016**, *37*, 3365–3372. [CrossRef]
42. Sanyang, M.L.; Sapuan, S.M.; Jawaid, M.; Ishak, M.R.; Sahari, J. Effect of plasticizer type and concentration on tensile, thermal and barrier properties of biodegradable films based on sugar palm (*Arenga pinnata*) starch. *Polymers* **2015**, *7*, 1106–1124. [CrossRef]
43. Anwer, M.A.S.; Naguib, H.E.; Celzard, A.; Fierro, V. Comparison of the thermal, dynamic mechanical and morphological properties of PLA-Lignin & PLA-Tannin particulate green composites. *Compos. Part B Eng.* **2015**, *82*, 92–99. [CrossRef]
44. Ferry, J.D. *Viscoelastic Properties of Polymers*; Wiley: Hoboken, NJ, USA, 1980; ISBN 9780471048947.
45. Rodriguez-Gonzalez, F.J.; Ramsay, B.A.; Favis, B.D. Rheological and thermal properties of thermoplastic starch with high glycerol content. *Carbohydr. Polym.* **2004**, *58*, 139–147. [CrossRef]
46. Lu, Y.; Weng, L.; Cao, X. Morphological, thermal and mechanical properties of ramie crystallites—Reinforced plasticized starch biocomposites. *Carbohydr. Polym.* **2006**, *63*, 198–204. [CrossRef]
47. Zanela, J.; Olivato, J.B.; Dias, A.P.; Grossmann, M.V.E.; Yamashita, F. Mixture design applied for the development of films based on starch, polyvinyl alcohol, and glycerol. *J. Appl. Polym. Sci.* **2015**, *132*, 43. [CrossRef]
48. Santana, R.F.; Bonomo, R.C.F.; Gandolfi, O.R.R.; Rodrigues, L.B.; Santos, L.S.; dos Santos Pires, A.C.; de Oliveira, C.P.; da Costa Ilhéu Fontan, R.; Veloso, C.M. Characterization of starch-based bioplastics from jackfruit seed plasticized with glycerol. *J. Food Sci. Technol.* **2018**, *55*, 278–286. [CrossRef]

49. Chakraborty, I.; Pooja, N.; Banik, S.; Govindaraju, I.; Das, K.; Mal, S.S.; Zhuo, G.Y.; Rather, M.A.; Mandal, M.; Neog, A.; et al. Synthesis and detailed characterization of sustainable starch-based bioplastic. *J. Appl. Polym. Sci.* **2022**, *139*, 1–12. [CrossRef]
50. Tunc, S.; Angellier, H.; Cahyana, Y.; Chalier, P.; Gontard, N.; Gastaldi, E. Functional properties of wheat gluten/montmorillonite nanocomposite films processed by casting. *J. Memb. Sci.* **2007**, *289*, 159–168. [CrossRef]
51. Álvarez-Castillo, E.; Felix, M.; Bengoechea, C.; Guerrero, A. Proteins from Agri-Food Industrial Biowastes or Co-Products and Their Applications as Green Materials. *Foods* **2021**, *10*, 981. [CrossRef] [PubMed]
52. Félix, M.; Martín-Alfonso, J.E.; Romero, A.; Guerrero, A.; Felix, M.; Martin-Alfonso, J.E.; Romero, A.; Guerrero, A. Development of albumen/soy biobased plastic materials processed by injection molding. *J. Food Eng.* **2014**, *125*, 7–16. [CrossRef]
53. Ferreira, W.H.; Carmo, M.M.I.B.; Silva, A.L.N.; Andrade, C.T. Effect of structure and viscosity of the components on some properties of starch-rich hybrid blends. *Carbohydr. Polym.* **2015**, *117*, 988–995. [CrossRef] [PubMed]